Mon. Not. R. Astron. Soc. **355,** 1303–1314 (2004) doi:10.1111/j.1365-2966.2004.08409.x

The cosmological significance of low surface brightness galaxies found in a deep blind neutral hydrogen survey

R. F. Minchin,[1⋆] M. J. Disney,[1] Q. A. Parker,[2] P. J. Boyce,[3] W. J. G. de Blok,[1] G. D. Banks,[1]† R. D. Ekers,[4] K. C. Freeman,[5] D. A. Garcia,[1] B. K. Gibson,[6] M. Grossi,[1] R. F. Haynes,[7] P. M. Knezek,[8] R. H. Lang,[1] D. F. Malin,[9] R. M. Price,[10] M. Putman,[11] I. M. Stewart[12] and A. E. Wright[4]

[1]*School of Physics and Astronomy, Cardiff University, 5 The Parade, Cardiff CF24 3YB*
[2]*Department of Physics, Macquarie University, Sydney, NSW 2109, Australia*
[3]*Planning Division, Cardiff University, Park Place, Cardiff CF10 3UA*
[4]*Australia Telescope National Facility, PO Box 76, Epping, NSW 1710, Australia*
[5]*Research School of Astronomy and Astrophysics, Mount Stromlo Observatory, Cotter Road, Weston, ACT 2611, Australia*
[6]*Centre for Astrophysics and Supercomputing, Swinburne University of Technology, PO Box 218, Hawthorn, Victoria 3122, Australia*
[7]*School of Mathematics and Physics, University of Tasmania, Hobart, Tasmania 7001, Australia*
[8]*WIYN Consortium Inc., 950 North Cherry Avenue, Tucson, AZ 85719, USA*
[9]*Anglo-Australian Observatory, PO Box 296, Epping, NSW 1710, Australia*
[10]*Department of Physics and Astronomy, University of New Mexico, 800 Yale Boulevard NE, Albuquerque, NM 87131, USA*
[11]*Department of Astronomy, University of Michigan, Ann Arbor, MI 48108, USA*
[12]*Department of Physics and Astronomy, University of Leicester, University Road, Leicester LE1 7RH*

Accepted 2004 September 12. Received 2004 August 20; in original form 2004 May 4

ABSTRACT

Minchin et al. have recently placed limits on the cosmological significance of gas-rich low surface brightness (LSB) galaxies as a proportion of the total population of gas-rich galaxies by carrying out a very deep survey (HIDEEP) for neutral hydrogen (H I) with the Parkes multibeam system. Such a survey avoids the surface brightness selection effects that limit the usefulness of optical surveys for finding LSB galaxies. To complement the HIDEEP survey, we have digitally stacked eight 1-h *R*-band Tech Pan films from the UK Schmidt Telescope covering 36 deg^2 of the survey area to reach a very deep isophotal limit of 26.5 *R* mag arcsec^{-2}. At this level, we find that all of the 129 H I sources within this area have optical counterparts and that 107 of them can be identified with individual galaxies. We have used the properties of the galaxies identified as the optical counterparts of the H I sources to estimate the significance of LSB galaxies (defined to be those at least 1.5 mag dimmer in effective surface brightness than the peak in the observed distribution seen in optical surveys). Two different methods of correcting for ease of detection do not yield significantly different results: LSB galaxies make up 62 ± 37 per cent of gas-rich galaxies by number according to our first method (weighting by H I mass function), which includes a correction for large-scale structure, or 51 ± 20 per cent when calculated by our second method ($1/V_{\rm max}$ correction). We also find that LSB galaxies provide 30 ± 10 per cent of the contribution of gas-rich galaxies to the neutral hydrogen density of the Universe, 7 ± 3 per cent of their contribution to the luminosity density of the Universe, 9 ± 4 of their contribution to the baryonic mass density of the Universe, 20 ± 10 per cent of their contribution to the dynamical mass density of the Universe, and 40 ± 20 per cent of their cross-sectional area. We do not find any 'crouching giant' LSB galaxies such as Malin 1, nor do we find a population of extremely low surface brightness galaxies not previously found by optical surveys. Such objects must be either rare, gas-poor or outside the survey detection limits.

⋆E-mail: Robert.Minchin@astro.cf.ac.uk
†Now at BAE Systems.

Key words: surveys – galaxies: fundamental parameters – galaxies: luminosity function, mass function – radio lines: galaxies.

1 INTRODUCTION

Surveys in the optical are known to be affected by strong selection effects (e.g. Disney 1976; Disney & Phillipps 1983; McGaugh 1996), which bias our understanding of the local galaxy population. Corrections for these selection effects can be made, but these are large and controversial and must be applied to small numbers of sources, leading to large uncertainties (Impey & Bothun 1997; Disney 1999). Low surface brightness (LSB) galaxies could make a significant contribution to the Universe that would not be recognized in an optical survey. They may dominate the luminosity, baryon or mass density of the galaxies in the Universe (e.g. Fukugita, Hogan & Peebles 1998) and could contribute significantly to quasar (QSO) absorption-line spectra (e.g. Churchill & Le Brun 1998).

Zwaan et al. (2003) derived the H I mass function for the 1000 galaxies in the H I Parkes All Sky Survey (HIPASS) Bright Galaxy Catalogue (Koribalski et al. 2004) and put a value of 15 per cent on the contribution of LSB galaxies to the neutral hydrogen density of the Universe. However, this number depends crucially on their assumption that optical catalogues are as (in)complete for LSB galaxies as for high surface brightness (HSB) galaxies. This is obviously not the case, as LSB galaxies are much harder to detect than HSB galaxies. Indeed, most of the new galaxies, outside of the zone of avoidance, found in the HIPASS Bright Galaxy Catalogue are LSB galaxies (Ryan-Weber et al. 2002). Thus the value of Zwaan et al. (2003) should be considered only a lower limit to the contribution of LSB galaxies to the neutral hydrogen density.

The idea of searching for galaxies via the 21-cm neutral hydrogen line has long been considered as an alternative to optical surveys (e.g. Disney 1976). However, until recent advances in technology such as multibeam receivers and powerful correlators, such a survey has not been practicable.

The HIDEEP survey (Minchin et al. 2003, hereafter Paper 1) was motivated by the desire to reach previously inaccessible surface brightness levels. If optical surface brightness (e.g. luminosity per square arcsecond) were to correlate with hydrogen column density (e.g. H I flux per square arcsecond), then to reach low surface brightnesses it would be necessary to reach low column densities. With an integration time of 9000 s beam^{-1}, HIDEEP is significantly more sensitive to low column density gas than any previous survey and thus potentially more sensitive to low surface brightness galaxies.

HIDEEP followed the same survey strategy and data reduction path as HIPASS (Barnes et al. 2001), but with 20 times the integration time. The Parkes multibeam system was actively scanned in declination to cover a 6×10 deg^2 region, with full sensitivity being reached over the central 4×8 deg^2. Scans were interleaved to give Nyquist sampling and repeated to reach the required depth. The data were treated in the same way as HIPASS data: they were reduced in AIPS++ using the LIVEDATA and GRIDZILLA programs, and continuum sources were removed by template fitting with the LUTHER program. In order to minimize the noise, all the observations were carried out at night. The full sensitivity reached was 3.2 mJy beam^{-1}, which is consistent with a $\sqrt{t}$ improvement on HIPASS.

To complement the deep H I data, we obtained eight 1-h exposures on Tech Pan films at the UK Schmidt Telescope (UKST). These covered a sky area of 6×6 deg^2, with the same centre as the H I survey data. The films were digitized using the SuperCOSMOS machine at the Royal Observatory, Edinburgh (Hambly et al. 2001). Digital stacking of these films brings a $\sqrt{t}$ improvement in signal-to-noise ratio (Bland-Hawthorn, Shopbell & Malin 1993), thus gaining us a little over a magnitude in depth. The use of Tech Pan films gives a further magnitude improvement over the III-aF *R*-band plates previously used at the UKST (Parker & Malin 1999). For galaxies with ordinary colours, our 1σ surface brightness limit of 26.5 *R* mag arcsec^{-2} is equivalent to $\sim$27.5 *B* mag arcsec^{-2}.

The bandpass limit of the multibeam system means that only objects with a heliocentric velocity less than 12 700 km s^{-1} can be detected [173 Mpc for $H_0 = 75$ km s^{-1} Mpc^{-1}, after correction to cosmic microwave background (CMB) rest-frame velocities]; thus the volume of the 36 deg^2 optical overlap region is 19 000 Mpc^3. Within this volume we find a total of 129 sources, of which 107 can be identified with individual galaxies.

2 ANALYSIS OF THE OPTICAL DATA

In Paper 1, we identified sources found in the H I data with optical counterparts on the Tech Pan films. A comparison of the offsets of the optical positions from the H I positions for the sources with secure identifications (those with catalogued velocities matching the H I velocity and those confirmed by H I interferometry or optical spectroscopy follow-up observations) with the offsets for less certain counterparts (those without catalogued velocities or follow-up observations) showed no significant difference. Of the 107 galaxies in this paper, 87 are secure identifications; this includes 18 confirmed with our interferometric follow-up and two with our spectroscopic follow-up. Of the remaining 20, 18 are previously catalogued galaxies that do not have redshifts in the literature and two are new detections.

An H I selected sample is expected to appear different from an optically selected one. In particular, low surface brightness galaxies – which are seen over much smaller volumes than high surface brightness galaxies with the same total luminosity in optical surveys (Disney & Phillipps 1983) – are expected to be seen much more easily. However, gas-poor galaxies, such as ellipticals and dwarf spheroidals, that are found by optical surveys will be invisible at 21 cm. We find that this is indeed the case with our sample. As expected, our surface brightness distribution (Fig. 1) is higher towards lower surface brightnesses than one finds in optically selected samples such as the ESO-LV (Lauberts & Valentijn 1989), which is also shown in the figure. A Kolmogorov–Smirnov test on our observed surface brightness distribution and the surface brightness distribution of the ESO-LV, which also uses *R*-band effective surface brightness, shows that the hypothesis that both are drawn from the same parent population has a significance of less than 1 per cent, as a result of the larger number of LSB galaxies seen in the HIDEEP sample. This confirms that H I surveys do, as expected, avoid some of the surface brightness selection effects present in optical surveys.

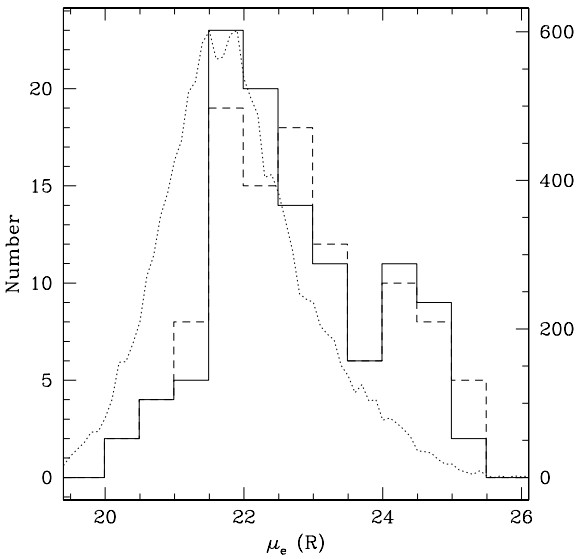

Figure 1. Number of galaxies found in each surface brightness bin. The solid line shows the distribution of observed surface brightnesses. The dashed line shows the distribution of surface brightnesses after correction for galactic absorption, cosmological dimming and inclination. The dotted line shows the observed surface brightness distribution of ESO-LV galaxies (right-hand scale).

2.1 Tabulated optical properties

Optical photometry of HIDEEP galaxies was carried out using a combination of SExtractor (Bertins & Arnouts 1996) and the STSDAS package in IRAF, where the ELLIPSE task was used to obtain radial surface brightness profiles. The measured optical parameters are displayed in Table 1 (a sample is shown here, with the full table being available at http://www.blackwellpublishing.com/products/journals/suppmat/MNR/MNR8409/MNR8409sm.htm), where column (1) gives the source name and (2) the catalogued identification – if there is one. Column (3) gives the type of the identification graded into three classes: 'ID' denotes objects where both positions and velocities coincide; 'PCG' (for previously catalogued galaxy) where there is a positional coincidence with a previously catalogued galaxy in the NASA Extragalactic Database (NED); and 'PUG' (for previously uncatalogued galaxy) where there is no possible counterpart in NED, and thus no previous positional or redshift data. Three further subclasses, 'ID-VLA', 'ID-ATCA' and 'ID-Spec', denote where a previously catalogued galaxy without a redshift has been confirmed as the optical counterpart through our follow-up observations (by interferometry with the VLA or the ATCA, or by spectroscopy at the ANU 2.3-m telescope at Siding Spring respectively).

The tabulated optical parameters are as follows. Column (4) gives the apparent magnitude m_R as measured by the mag_best parameter in SExtractor. This takes the form of either an adaptive aperture magnitude (Kron 1980), where the size of the aperture is 2.5 times the first-moment radius of the galaxy, or, for crowded fields, an isophotal magnitude (to the 26 R mag arcsec^{-2} isophote) with a correction made for the part of the galaxy beyond the isophotal limit (Maddox, Efstathiou & Sutherland 1990), the best algorithm being selected automatically by the program. Simulations by Bertins & Arnouts (1996) of an R-band charge-coupled device (CCD) image with an isophotal limit of 26 R mag arcsec^{-2} (i.e. very similar to our image) show that, to the magnitude level of the faintest galaxy in our survey (18.6 R mag), the true magnitude is recovered to better than 0.1 mag.

Column (5) gives the effective radius r_e – the radius enclosing half the R-band light. Column (6) gives the effective surface brightness μ_e – the R-band surface brightness at the effective radius. This gives a model-independent measure of the surface brightness, which can be applied to all types of galaxies. Column (7) gives the SExtractor ellipticity ($\epsilon = 1 - b/a$) and column (8) the estimated R-band absorption at the position of the object from Schlegel, Finkbeiner & Davis (1998) supplied by NED. Column (9) gives the absolute magnitude M_R, including corrections for Galactic absorption, cosmological dimming and internal absorption [estimated using $A_{i,R} = 0.95 \log(a/b)$, where a/b is calculated from ϵ]. The k-correction out to the bandpass limit of 12 700 km s^{-1} is negligible. We use the distances from Paper 1 except for galaxies in the Centaurus A group (taken to be those within 1000 km s^{-1}), where we use the distance to the M83 subgroup of 4.5 Mpc from Thim et al. (2003). Column (10) gives the physical effective radius R_e in kpc. Finally column (11) gives the surface brightness μ_e(c) corrected for $(1 + z)^4$ cosmological dimming, inclination [estimated using $C_{i,R} = -1.25 \log(a/b)$ from Graham & de Blok 2001] and galactic absorption.

Table 2 gives the positions of the optical counterparts of the PUGs. Where these have been confirmed by interferometric follow-up, this is indicated by a code in column (4) giving the run in which they were detected. The PUGs that were not detected in earlier runs were followed up again in later runs, with the result that there are no galaxies in the table that have been followed up but not detected, although there are two sources that have not been followed up interferometrically.

3 VOLUMETRIC AND LARGE-SCALE STRUCTURE CORRECTED DATA

No conclusions can be drawn as to the cosmic significance of the LSB galaxies found in HIDEEP until the raw numbers have been corrected for ease of H I detection and for the large-scale structure in the region. The peak flux (S_{peak}) of a galaxy determines the distance to which it may be seen in an H I survey and is related to its H I mass (M_{HI}) and its velocity width (ΔV) as $M_{HI} \propto d^2\, \Delta V\, S_{peak}$. However, the velocity width is not independent of the mass of a galaxy – these are related as $\Delta V \propto M_{HI}^{1/3}$ (Briggs & Rao 1993); thus $M_{HI} \propto d^3\, S_{peak}^{3/2}$. For a fixed limiting peak flux, we therefore get $M_{HI,lim} \propto d^3$. While this is an approximate empirical relationship originally defined using an optically selected sample of galaxies, the general result that higher H I mass galaxies can be seen to greater distances is found to hold true in blind H I surveys (e.g. Zwaan et al. 1997 or Koribalski et al. 2004). The exact form of this dependence of limiting H I mass on distance is not used in our analysis and is thus unimportant for the purposes of this study.

We find that parameters such as absolute magnitude and surface brightness are correlated with hydrogen mass (Figs 2 and 3). Thus more luminous galaxies may be seen over larger volumes and, in a reversal of the situation in the optical, low surface brightness galaxies may be seen over larger volumes than higher surface brightness galaxies of the same luminosity due to the anticorrelation between surface brightness and the H I mass-to-light ratio (Fig. 4) seen both in our data and in previous studies using optically selected samples (e.g. de Blok, McGaugh & van der Hulst 1996).

In order to make the volumetric corrections for H I selection effects, we use two different methods, which are described below. We have chosen to remove dwarf galaxies ($M_{HI} < 10^8\, M_\odot$) from this analysis for two main reasons: that the number of low-mass galaxies in our sample is low, and that the volume in which we can see

Table 1. Optical properties of HIDEEP galaxies. The full version of this table is available from http://www.blackwellpublishing.com/products/journals/suppmat/MNR/MNR8409/MNR8409sm.htm .

ID	Catalogue	Class	m_R	r_e (arcsec)	μ_e ($R\mu$)	ϵ	A_R	M_R	R_e (kpc)	μ_e(c) ($R\mu$)
(1)	(2)	(3)	(4)	(5)	(6)	(7)	(8)	(9)	(10)	(11)
HIDEEP J1326−3024	IC 4247	ID	13.8	16.7	22.4	0.57	0.17	−15.0	0.98	22.7
HIDEEP J1326−3209	ESO 444-G033	ID-VLA	14.0	23.9	22.4	0.74	0.14	−19.5	4.2	23.0
HIDEEP J1327−2713	ESO 509-G014	PCG	16.5	4.3	22.4	0.40	0.15	−16.5	0.72	22.5
HIDEEP J1327−2935	NGC 5150	ID	12.4	11.7	20.9	0.24	0.15	−21.6	3.1	20.8
HIDEEP J1327−3006	UGCA 358	ID	14.5	21.7	24.4	0.56	0.16	−18.4	3.1	24.7
HIDEEP J1328−2735	ESO 509-G026	ID	16.5	7.3	24.1	0.32	0.14	−16.1	1.0	24.1
HIDEEP J1328−2819	[BZZ2000] J132823.03−2811814.7	ID	16.6	8.0	24.0	0.34	0.14	−16.4	1.3	24.1
HIDEEP J1328−3152	ESO 444-G047	ID	13.7	12.7	22.1	0.65	0.14	−20.8	3.8	22.5
HIDEEP J1329−2714	ESO 509-G031	PCG	17.3	9.7	25.3	0.10	0.15	−16.4	2.4	25.2
HIDEEP J1329−3144	Abell 3558: [MGP94] 2773	ID-VLA	18.1	5.2	24.1	0.20	0.14	−16.2	1.6	24.0
HIDEEP J1329−3203	ESO 444-G056	ID	16.3	7.3	23.4	0.12	0.13	−18.0	2.3	23.2
HIDEEP J1330−2755	IC 4264	ID	14.2	10.7	22.2	0.60	0.14	−19.8	2.6	22.5
HIDEEP J1330−2809	NGC 5182	ID	12.0	30.0	22.0	0.53	0.15	−22.5	9.0	22.2
HIDEEP J1330−2936	2MASX J13303473−2934210	ID-VLA	14.6	11.6	23.1	0.52	0.15	−19.6	3.1	23.3
HIDEEP J1330−3212	ESO 444-G059	PCG	16.8	12.1	25.1	0.11	0.14	−17.2	3.3	25.0
HIDEEP J1330−3233	ESO 444-G061	PCG	14.8	10.7	23.2	0.07	0.14	−21.5	8.4	22.9
HIDEEP J1330−3259		PUG	14.9	26.7	24.8	0.45	0.15	−19.1	7.9	24.9
HIDEEP J1331−2804	[QRM95] 1325−27 50	ID	13.6	8.0	21.4	0.24	0.15	−22.4	5.4	21.6
HIDEEP J1331−2944	IC 4275	ID	13.1	11.4	21.3	0.39	0.15	−21.2	3.4	21.3
HIDEEP J1331−3155	ESO 444-G066	ID	14.9	11.6	23.7	0.09	0.14	−19.3	3.6	23.6
HIDEEP J1331−3205	Abell 3558: [MGP94] 3325	PCG	16.9	6.6	23.9	0.35	0.13	−15.7	0.90	24.0
HIDEEP J1331−3258	GSC 7269 01680	ID	14.4	7.3	22.0	0.34	0.15	−19.5	1.8	22.0
HIDEEP J1332−2727	ESO 509-G048	ID	14.0	9.3	22.5	0.10	0.17	−22.3	6.6	22.4
HIDEEP J1332−3141	Abell 3558: [MGP94] 3535	ID	15.7	9.3	23.5	0.09	0.14	−20.4	6.6	23.3
HIDEEP J1333−2727	IRAS F13304−2714	PCG	16.3	4.5	22.9	0.35	0.18	−19.9	3.1	22.8
HIDEEP J1333−2743	IC 4286	PCG	15.0	5.2	21.9	0.11	0.17	−20.9	3.4	21.7
HIDEEP J1333−2901	[DPP99] 13300.7−284540	ID	15.6	10.7	22.8	0.62	0.15	−19.5	4.1	23.0
HIDEEP J1333−3158	ESO 444-G070	ID	14.0	8.4	21.9	0.20	0.14	−22.2	6.2	21.7
HIDEEP J1333−3243	ESO 444-G071	ID	13.4	15.9	21.6	0.68	0.15	−21.1	4.6	22.0

these galaxies in dominated by the Centaurus A group. For these reasons, we focus solely on the more H I massive galaxies ($M_{HI} > 10^8\,M_\odot$), where we have reasonable statistics and probe a variety of environments.

Table 2. Positions of newly discovered galaxies in the HIDEEP optical area. For those detected interferometrically, column (4) gives the code for the observing run: A1 – ATCA, 1999/11; A2 – ATCA, 2000/01; V – VLA, 2003/01–03; A3 – ATCA, 2003/04. Those without a code have not been observed with an interferometer.

HIDEEP ID	RA	Dec.	Run
(1)	(2)	(3)	(4)
J1330−3259	13:30:32	−32:57:07	V
J1336−2932	13:36:08	−29:34:12	A1
J1337−3118	13:36:59	−31:19:05	V
J1338−3035	13:37:56	−30:35:12	A2
J1339−3022	13:39:08	−30:22:10	V
J1342−2859	13:42:05	−29:01:21	A2
J1342−3021	13:42:21	−30:23:14	V
J1344−3202	13:44:03	−32:02:11	–
J1345−2908	13:45:30	−29:06:47	V
J1345−3041	13:45:20	−30:43:21	–
J1345−3104	13:45:12	−30:56:52	V
J1347−2735	13:47:37	−27:35:22	V
J1347−2810	13:47:45	−28:11:56	A3
J1348−2856	13:48:38	−29:00:22	V

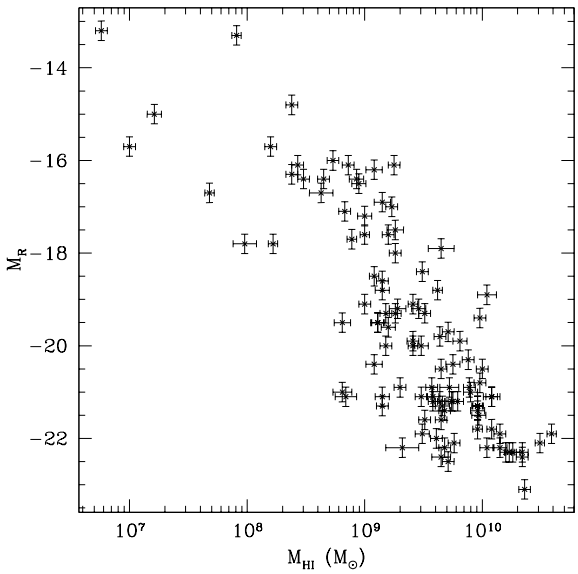

Figure 2. Relationship between H I mass and absolute magnitude.

3.1 $1/V_{max}$ weighting

Weighting detections by $1/V_{max}$, where V_{max} is the total volume in which they could have been found, is well established as a means of

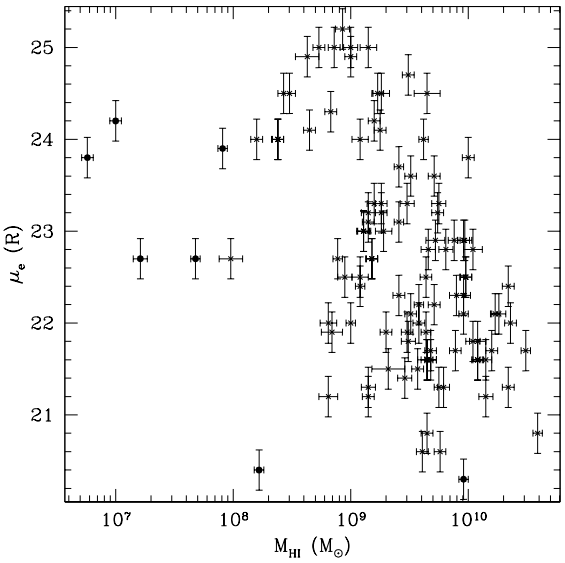

Figure 3. Relationship between H I mass and effective surface brightness. Cen A group galaxies are shown by solid circles. The relationship is weaker than for luminosity, but there is a definite trend for lower H I mass galaxies to have lower surface brightnesses: 14 of the 23 galaxies with $M_{\rm HI} < 10^9\,{\rm M}_\odot$ are LSB galaxies ($\mu_{\rm e}(R) > 23.3$ R mag arcsec^{-2}), while, at the high-mass end, there is only one LSB galaxy out of the 16 with $M_{\rm HI} > 10^{10}\,{\rm M}_\odot$. This dependence of surface brightness on H I mass means that corrections must be made for H I selection effects before the surface brightness distribution can be determined.

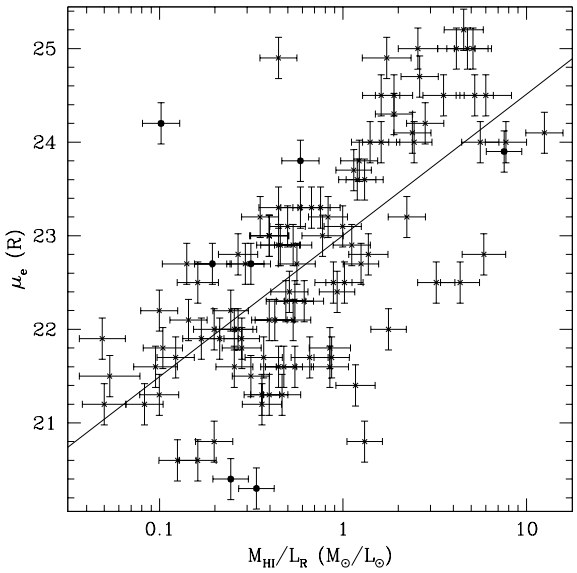

Figure 4. Correlation of effective surface brightness with H I mass-to-light ratio. Cen A group galaxies are shown by solid circles. The correlation between $\mu_{\rm e}$ and $\log(M_{\rm HI}/L_R)$, shown as a solid line, has a slope of 1.51 ± 0.16 and a scatter of 0.9 mag. As the survey detects galaxies by their H I content, galaxies with low H I mass-to-light ratios may be missed; however, this survey goes deep enough to see galaxies down to $M_{\rm HI}/L_R \simeq 0.05\,{\rm M}_\odot/{\rm L}_\odot$, so it is unlikely that this will be a significant effect.

correcting for ease of detection. We use this here with a completeness limit of 18 mJy in peak flux (Paper 1) and a maximum distance, due to the bandpass limit of the H I survey, of 173 Mpc. This gives us a complete sample of 67 galaxies with $\langle V/V_{\rm max}\rangle = 0.49 \pm 0.04$. Once the dwarfs are removed, we are left with 62 galaxies with $\langle V/V_{\rm max}\rangle = 0.52 \pm 0.04$. While $1/V_{\rm max}$ is well understood, it cannot make any correction for the large-scale structure, which could lead to distortions in the results. However, the value of $\langle V/V_{\rm max}\rangle$ implies that the overall effect of large-scale structure on the sample is probably not large.

3.2 H I mass function weighting

Our second method is to use an H I mass function (HIMF) to correct for both ease of detection and large-scale structure, as described in Minchin (1999). This method makes the assumption that our galaxies are drawn from the same population as a general HIMF, such as that found for the HIPASS Bright Galaxy Catalogue (BGC) by Zwaan et al. (2003). Then the volumetric correction that needs to be applied in order to match the distribution of H I masses in HIDEEP with the HIMF can be calculated and applied to find other quantities, such as the luminosity function and the surface brightness distribution. After dwarf galaxies are excluded, this gives us a sample of 101 galaxies.

This HIMF weighting cannot be used to construct an H I mass function for the HIDEEP galaxies, as it would clearly just give the same answer as the input HIMF. However, we can use it to construct the bivariate brightness distribution, luminosity function and surface brightness distribution of galaxies and to investigate how various parameters (e.g. luminosity density) change with surface brightness. It would be possible to make a HIMF from the HIDEEP data using $1/V_{\rm max}$; however, we have chosen to use the HIMF of Zwaan et al. (2003), based on the 1000 galaxies in the HIPASS BGC. This contains an order of magnitude more galaxies than HIDEEP and thus gives a much more accurate mass function.

HIMF weighting contains more sources of error than $1/V_{\rm max}$. The main sources of additional errors are the width of the bins used in the HIMF and the numbers of galaxies in each bin. The resulting formal uncertainties are therefore normally larger than for $1/V_{\rm max}$, despite the larger sample size. However, it should be remembered that HIMF weighting includes a correction for the large-scale structure that is not factored into either the values or the errors of the $1/V_{\rm max}$ weighting.

Systematic errors may be introduced by the choice of the HIMF. In order to gauge the size of these errors, we have looked at the contribution of LSB galaxies to the total number density of gas-rich galaxies when calculated with the HIMFs of Rosenberg & Schneider (2002), Kilborn (2001), Henning et al. (2000) and Zwaan et al. (1997) (see Table 3 for a summary). The resulting surface brightness distributions are shown in Fig. 5.

It can be seen from Fig. 5 that there is little difference in the overall shape of the surface brightness distributions derived using the different HIMFs, although the overall density of gas-rich galaxies is significantly reduced if the HIMF of Zwaan et al. (1997) is used. The contribution of LSB galaxies as a proportion of all galaxies is therefore only weakly dependent on the HIMF chosen, with a

Table 3. H I mass functions used in calculating the weighting (corrected to $H_0 = 75$ km s^{-1} Mpc^{-1}).

α	$\phi^\star$	$\log M^\star_{\rm HI}$	Ref.
−1.30	0.0086	9.79	Zwaan et al. (2003) (BGC)
−1.53	0.005	9.88	Rosenberg & Schneider (2002)
−1.52	0.0032	10.1	Kilborn (2001)
−1.51	0.006	9.7	Henning et al. (2000)
−1.2	0.006	9.8	Zwaan et al. (1997)

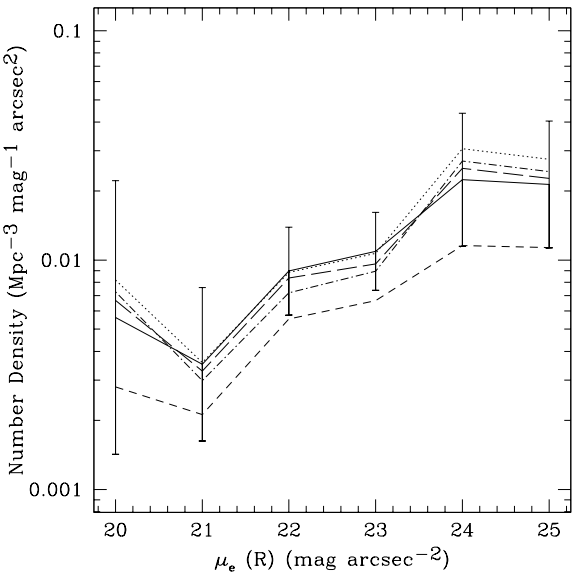

Figure 5. The surface brightness distribution formed by correcting with various different H I mass functions: solid line, HIPASS Bright Galaxy Catalogue (BGC; Zwaan et al. 2003) as used elsewhere in this paper; dotted line, Rosenberg & Schneider (2002); short-dashed line, Zwaan et al. (1997); long-dashed line, Kilborn (2001); dot-dashed line, Henning et al. (2000). Error bars are given for the distribution formed using the BGC HIMF.

slight rise in the proportion for steeper slopes. Within the range of HIMFs here, the proportion of LSB galaxies varies between 59 and 67 per cent of all gas-rich galaxies, with the BGC HIMF giving 62 per cent. As the statistical error on this proportion is 37 per cent, it can be seen that the systematic error due to the HIMF is comparatively small. These systematic errors are stated in Table 4 as a second error column to the percentage LSB contribution.

Masters, Haynes & Giovanelli, (2004) have shown that, if a peculiar velocity field model is used to assign distances to galaxies in the BGC rather than the pure Hubble law used by Zwaan et al. (2003), then the faint-end slope of the BGC HIMF steepens from $\alpha = -1.3$ to -1.4, which is consistent with the steeper determinations. The HIMF of Zwaan et al. (1997) is also inconsistent with the other determinations; this cannot be explained by the method used for assigning distances but may be due to problems with correctly determining the survey sensitivity (Schneider, Spitzak & Rosenberg 1998). It is most likely, therefore, that if a systematic error has been introduced by the use of the HIMF, it is that the faint-end slope we have used is too shallow. The result of this would be for this paper to underestimate slightly the contribution of LSB galaxies.

3.3 The bivariate brightness distribution

As luminosity and surface brightness appear to be correlated to some degree, the distributions of luminosity and surface brightness on their own are less interesting than the bivariate brightness distribution (BBD) – the joint distribution in the (M_R, μ_e^R) plane. The BBD describes the contribution of galaxies of different luminosities and surface brightnesses to the cosmos, but is virtually impossible to obtain accurately from an optically selected sample (Boyce & Phillipps 1995). For instance, the largest sample of galaxies, complete in both surface brightness and luminosity, that can be assembled from the classical optical catalogues numbers less than 50 (Disney 1999).

Fig. 6 shows the BBDs drawn from the uncorrected samples, showing the correlation between luminosity and surface brightness

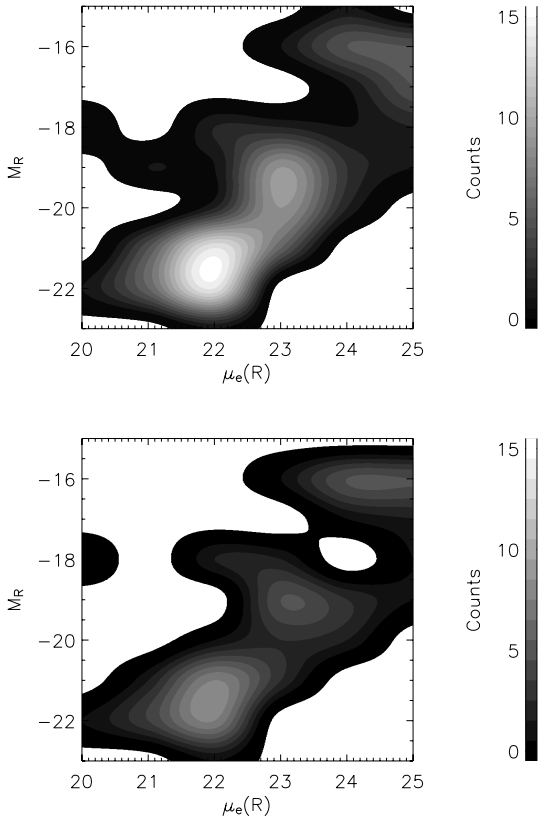

Figure 6. Uncorrected bivariate brightness distribution of HIDEEP galaxies. The upper panel shows the 101 galaxies in the HIMF-weighted sample, the lower panel the 62 galaxies in the $1/V_{\rm max}$-weighted sample. The blank areas around the images indicate where there is no data.

and illustrating the conventional emphasis on the overwhelming importance of high surface brightness giant galaxies. However, these galaxies tend to have much larger H I masses and can be seen over much greater volumes.

The corrected BBDs, showing the true space density of galaxies, are given in Fig. 7. The HIMF and $1/V_{\rm max}$ corrections give very similar results. Over a range of seven magnitudes in luminosity and five in surface brightness, the galaxies appear to lie in an evenly populated strip four magnitudes wide in luminosity and two in surface brightness that stretches from high luminosity, high surface brightness to low luminosity, low surface brightness.

The HIMF-weighted BBD is obviously dependent on the HIMF used to construct it. However, all of the HIMFs in Table 3 give results fairly similar to those shown here: if a steeper HIMF is used, then the density at low luminosity, low surface brightness is marginally higher; while if the shallower (and lower-density) HIMF of Zwaan et al. (1997) is used, then the density decreases all round, with the density of low-luminosity, low surface brightness galaxies falling slightly more than that of high-luminosity, high surface brightness galaxies.

We define LSB galaxies to be those with effective *R*-band surface brightnesses more than 1.5 mag lower than the peak in the uncorrected *R*-band effective surface brightness distribution of ESO-LV galaxies, i.e. $\mu_e(R) > 23.3$ mag arcsec^{-2}. This is slightly dimmer than the definitions used by Impey & Bothun (1997) [$\mu_0(B) > 23$] and by McGaugh (1996) [$\mu_0(B) > 22.75$], which are respectively 1.35 and 1.1 mag dimmer than the peak in the uncorrected *B*-band central surface brightness found by Freeman (1970). Using our

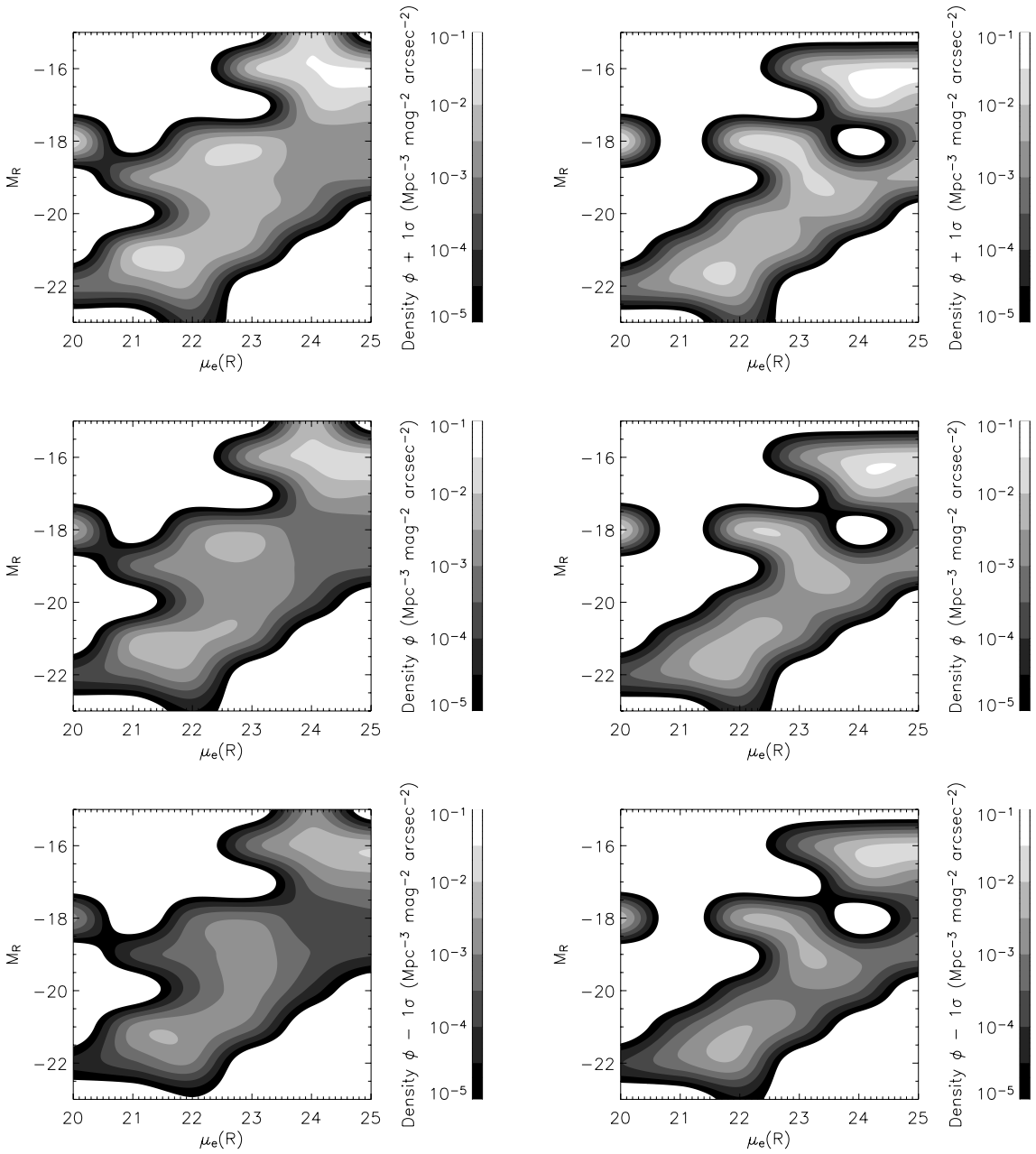

Figure 7. The bivariate brightness distributions of H I-selected galaxies. The panels to the left show the BBD formed using HIMF weighting, as described above, while the panels to the right show the BBD formed using $1/V_{\rm max}$ weighting. The central panels give the best estimate of the BBD, whereas the top panels show the BBD + 1σ in each bin and the bottom panels show the BBD − 1σ in each bin.

definition, we can set limits on the population of giant LSB galaxies as follows.

There is a clear deficiency of high-luminosity, LSB 'crouching giant' galaxies (LSB galaxies with $L_R > 10^{10}\,{\rm L}_\odot$): of the 47 galaxies with $L_R > 10^{10}\,{\rm L}_\odot$, not one is an LSB galaxy. By applying the binomial theorem, we can calculate that the probability of finding no LSB galaxies in a sample of 47 is less than 0.05 if LSB galaxies make up more than 6 per cent of the population. We can therefore rule out that LSB galaxies make up more than 6 per cent of the high-luminosity, gas-rich population with 95 per cent confidence.

Of the 16 H I massive ($M_{\rm HI} > 10^{10}\,{\rm M}_\odot$) galaxies found in HIDEEP, one (ESO 383-G059) is an LSB galaxy with $\mu_e^R = 23.8\ R\mu$ – this galaxy has a high H I mass despite not having a high optical (R-band) luminosity. By the same method as above, we can place a limit on the proportion of H I massive galaxies that are LSB galaxies of 26 per cent at the 95 per cent confidence level.

There is little evidence that the unpopulated regions at high luminosity, low surface brightness and low luminosity, high surface brightness are due to the H I mass limits of the survey (imposed by the downturn in the H I mass function at high $M_{\rm HI}$ and by small volumes, and the cut at $10^8\,{\rm M}_\odot$, at low $M_{\rm HI}$). Only one of the galaxies with $M_{\rm HI} > 10^{10}\,{\rm M}_\odot$ is a low surface brightness galaxy, as previously noted, and the high-mass galaxies are not spread along the high-luminosity edge of the populated region as would be expected if this edge were due to an H I mass selection effect. Similarly, only

one of the galaxies in the lowest mass range included in the sample ($10^{8.5}\,M_\odot > M_{HI} > 10^8\,M_\odot$) is a high surface brightness galaxy (NGC 5253); these galaxies are not spread along the low-luminosity edge of the populated region.

The dwarf galaxies that were removed from the sample ($M_{HI} < 10^8\,M_\odot$) fall in the surface brightness range 22.5–24.5 *R* mag arcsec^{-2} and in the *R* magnitude range −13 to −18, generally at a lower luminosity than is 'normal' for their surface brightness. All but one of these galaxies (all in the $1/V_{max}$ sample) lie in the Cen A group and are not, therefore, representative of a variety of environments – the one dwarf that is not in the Cen A group (HIDEEP J1337−3118) lies well within the normal range of luminosity for its surface brightness, while the higher-mass galaxy NGC 5253, which also lies in the Cen A group, is the galaxy most underluminous for its surface brightness in the sample. Including these dwarf galaxies in the BBD would not populate in the low-luminosity, high surface brightness region, but would extend the BBD to lower luminosities at intermediate and low surface brightnesses.

By collapsing the BBD along the surface brightness axis, we can form the optical luminosity function (LF), which is shown in Fig. 8. This is compared to the LF obtained by Blanton et al. (2001) from Sloan Digital Sky Survey (SDSS) commissioning data. It can be seen that both the HIMF and $1/V_{max}$ determinations are fairly consistent with the SDSS luminosity function, although $M_\star$ appears to be marginally brighter in our data – this could be due to uncertainties in the conversion between $r^\star$, which Blanton et al. use, and *R*. The $1/V_{max}$ weighting gives a faint-end ($M_R > -21.5$) slope of $\alpha = -1.40 \pm 0.14$ and the HIMF weighting gives $\alpha = -1.27 \pm 0.16$.

Fig. 9 displays the surface brightness distribution (SBD), formed by collapsing the BBD along the luminosity axis. This is consistent with optical determinations such as Davies (1990) and de Jong (1996a). The effect of large-scale structure on $1/V_{max}$ can be seen in the brightest bin. Both of the galaxies in this bin lie in the close by Cen A group and their contribution to the density is therefore overestimated by this method. However, in general the $1/V_{max}$ and HIMF weighted points are in good agreement, giving confidence that large-scale structure is not overly affecting the $1/V_{max}$ data.

Overall, it can be seen that optical surveys give very similar results to this survey. This implies that 21-cm surveys do not uncover any 'hidden' population of extremely low surface brightness galaxies that is missed by optical surveys. If such a population does exist in significant numbers, it must be composed primarily of galaxies with neutral gas masses lower than $10^8\,M_\odot$.

This is not to say, however, that LSB galaxies do not make up a significant population. The SBD derived from weighting by the BGC HIMF implies that LSB galaxies make up 62 ± 37 per cent of the total population of galaxies with $M_{HI} > 10^8\,M_\odot$, or 51 ± 20 per cent for $1/V_{max}$ weighting. Even with the large errors on these estimates, it is clear that a large number of galaxies fall into our definition of low surface brightness. In the next section we investigate what contribution these LSB galaxies make to the Universe.

4 THE COSMOLOGICAL SIGNIFICANCE OF LOW SURFACE BRIGHTNESS GALAXIES

As LSB galaxies have been proposed as repositories for some of the missing baryons (e.g. Impey & Bothun 1997) and may also contain large quantities of dark matter, it is important to make an estimate of how much they actually contribute to the Universe. It is possible to do this from our data, subject to the provisos that H I-poor galaxies would not be found at 21 cm (e.g. elliptical galaxies) and that we do not detect sufficient numbers of dwarf galaxies ($M_{HI} < 10^8\,M_\odot$) to say anything about their contribution. We compare the contribution of the LSB galaxies in our sample to the total contribution of H I-rich galaxies using the weightings described in Section 3 to correct the numbers in each surface brightness bin.

To compare the contribution to the luminosity density made by galaxies of different surface brightnesses, we need to weight the surface brightness distribution in Fig. 9 with the luminosities of the galaxies. When this is done we obtain Fig. 10, which shows

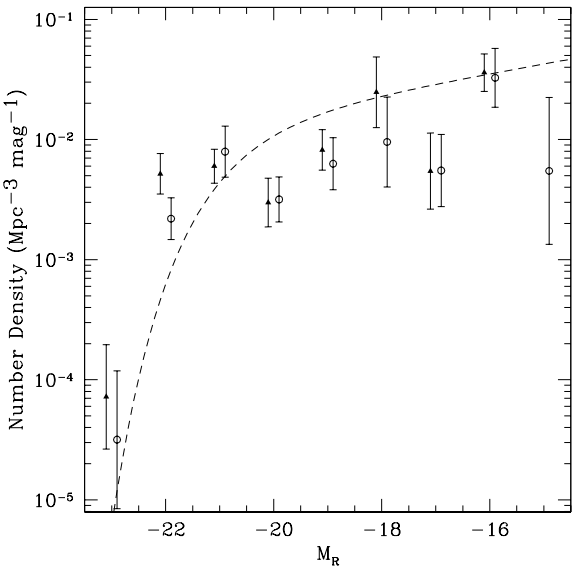

Figure 8. Weighted luminosity function of HIDEEP galaxies. Points weighted by the HIMF are shown as open circles (offset for clarity by 0.1 mag dimmer), and points weighted by $1/V_{max}$ are shown as solid triangles (offset for clarity by 0.1 mag brighter). The LF of Blanton et al. (2001), $\alpha = -1.20 \pm 0.03$, is shown as a dashed line.

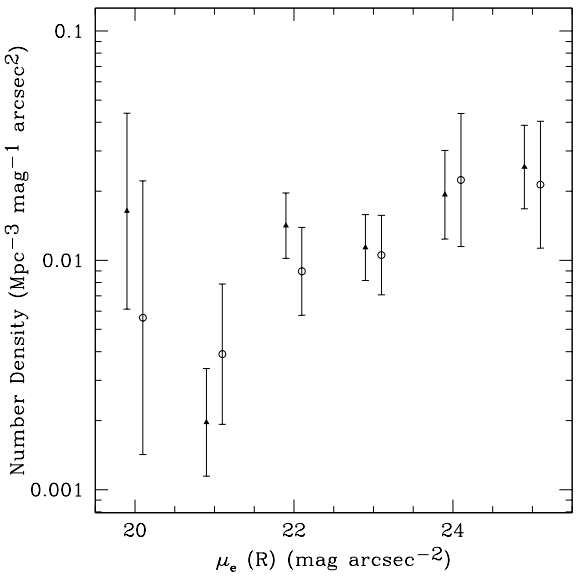

Figure 9. Corrected surface brightness distribution of HIDEEP galaxies. This is consistent with a flat or slowly rising surface brightness distribution at lower surface brightnesses and a downturn at the bright end. The HIMF-weighted points are indicated by open circles (offset for clarity by 0.1 mag dimmer), and the $1/V_{max}$-weighted points by solid triangles (offset for clarity by 0.1 mag brighter).

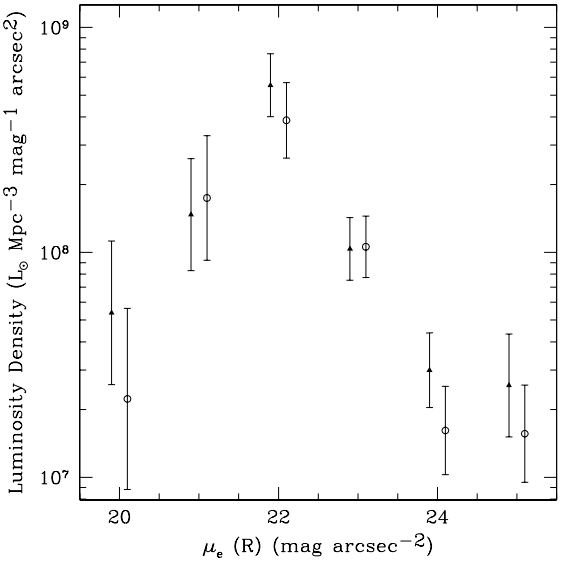

Figure 10. Luminosity density–surface brightness distribution for HIDEEP galaxies. The luminosity density can be seen to fall sharply either side of a peak near the Freeman-law value. The HIMF-weighted points are indicated by open circles (offset for clarity by 0.1 mag dimmer) and the $1/V_{\rm max}$-weighted points by solid triangles (offset for clarity by 0.1 mag brighter).

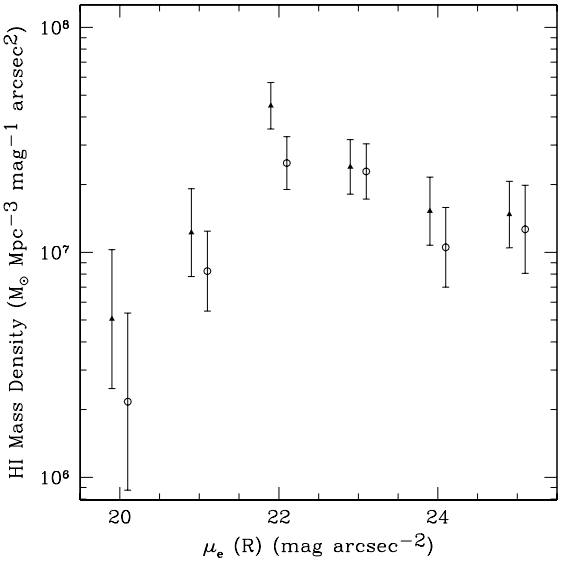

Figure 11. Neutral hydrogen density–surface brightness distribution for HIDEEP galaxies. It can be seen that this is consistent with a slowly falling distribution towards lower surface brightnesses and a much steeper fall-off towards higher surface brightnesses, similar in shape to the surface brightness distribution. The HIMF-weighted points are indicated by open circles (offset for clarity by 0.1 mag dimmer) and the $1/V_{\rm max}$-weighted points by solid triangles (offset for clarity by 0.1 mag brighter).

that the luminosity density is sharply peaked near the Freeman-law value. Gas-rich LSB galaxies do not appear to emit much light: when analysed with the HIMF weighting, they contribute 6.7 ± 2.8 per cent of the total luminosity density of all gas-rich galaxies, or 6.5 ± 2.4 per cent according to the $1/V_{\rm max}$ analysis. This is very similar to the 7.3 ± 3.6 per cent contribution for LSB galaxies found by Driver (1999) for local ($0.3 < z < 0.5$) galaxies in the *Hubble Deep Field*. The main source of errors in our determination is Poisson noise in the surface brightness bins, but there is also a contribution due to the uncertainty on the luminosity of the sources and, for the H I mass function weighting, due to the width of the mass bins and the number of galaxies in each bin.

Similarly the contribution of LSB galaxies to the H I content as a whole can be calculated and is shown in Fig. 11. This amounts to 32 ± 11 per cent of all H I with HIMF weighting, or 27 ± 7 per cent with $1/V_{\rm max}$ weighting.

This is inconsistent, at the 1σ level, with the determination of Zwaan et al. (2003) that LSB galaxies contribute only 15 per cent to the total H I mass density. That determination should, however, be treated as a lower limit. The sample of Zwaan et al., unlike our sample, did not have complete optical data – surface brightnesses were only available for 600 out of the 1000 galaxies. When corrections for this were made, Zwaan et al. assumed that the incompleteness in the optical data was unrelated to surface brightness. It is far more likely that the LSB galaxies' data were more incomplete than the HSB galaxies' data, which could raise the contribution of LSB galaxies considerably.

The baryonic content of the galaxies was calculated following the method of McGaugh et al. (2000), adding the mass of the stars and the gas together to get a total baryonic mass for the galaxy:

$$M_{\rm bary} = 1.4 M_{\rm H\,I} + \Upsilon^X_\star L_X, \quad (1)$$

where $\Upsilon^X_\star$ is the stellar mass-to-light ratio in the band used, and L_X is the luminosity in that band. For our R-band data, $\Upsilon^R_\star$ has been estimated, as in McGaugh et al., using the model of de Jong (1996b) for a 12 Gyr old, solar-metallicity stellar population with a constant

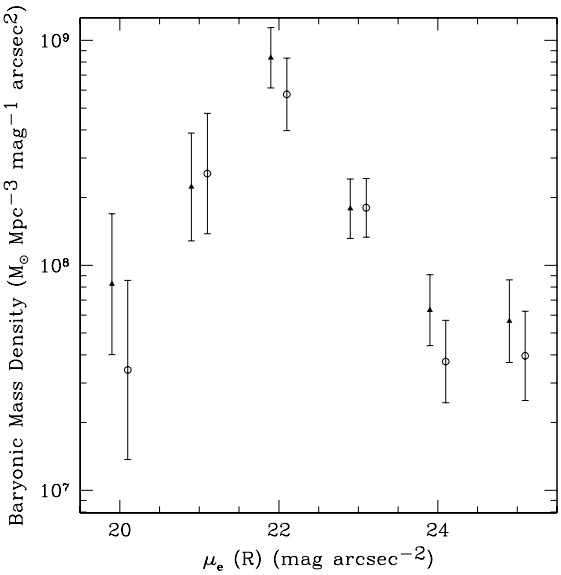

Figure 12. Baryon density–surface brightness distribution for HIDEEP galaxies. It can be seen that the greatest contribution to the baryon density is made by Freeman-law galaxies around $\mu^\star_e$, with the density falling off towards lower and higher surface brightnesses. The HIMF-weighted points are indicated by open circles (offset for clarity by 0.1 mag dimmer) and the $1/V_{\rm max}$-weighted points by solid triangles (offset for clarity by 0.1 mag brighter).

star formation rate and a Salpeter initial mass function, corrected to R band using the average colours in that paper (also used by McGaugh et al. for their correction to H band). This gives a value of $\Upsilon^R_\star \approx 1.4$, which we have used in our calculations.

The relative contribution of LSB galaxies to the total baryon density (shown in Fig. 12) is then calculated to be 9.3 ± 3.6 per cent

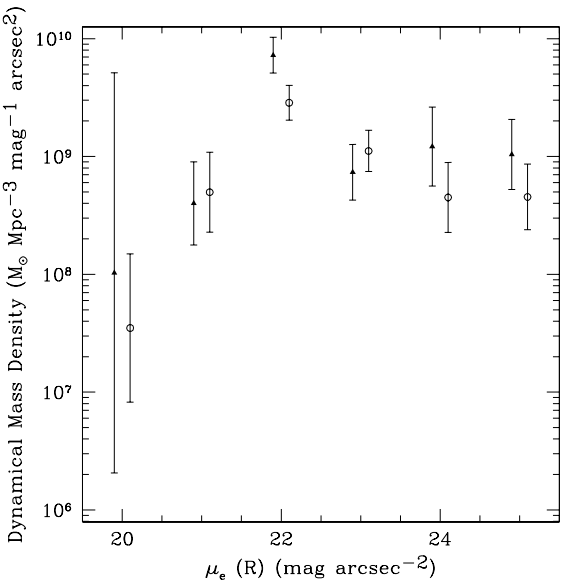

Figure 13. Mass density–surface brightness distribution for HIDEEP galaxies. The greatest contribution is made by Freeman-law galaxies $\mu_c^\star$. However, the distribution seems fairly flat towards lower surface brightnesses, while it falls off towards higher surface brightnesses. The HIMF-weighted points are indicated by open circles (offset for clarity by 0.1 mag dimmer) and the $1/V_{\rm max}$-weighted points by solid triangles (offset for clarity by 0.1 mag brighter).

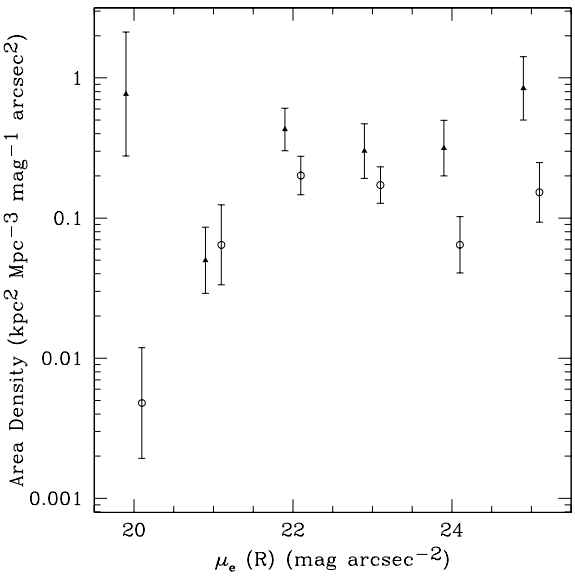

Figure 14. Cross-sectional area density against surface brightness for HIDEEP galaxies. This is fairly flat, with a fall-off towards higher surface brightnesses (the brightest point of the $1/V_{\rm max}$ distribution is, as noted earlier, affected by large-scale structure). This implies that LSB galaxies will make a significant contribution to quasar absorption lines insofar as these are caused by galaxies. The HIMF-weighted points are indicated by open circles (offset for clarity by 0.1 mag dimmer) and the $1/V_{\rm max}$-weighted points by solid triangles (offset for clarity by 0.1 mag brighter).

using HIMF weighting or 8.7 ± 2.9 per cent using $1/V_{\rm max}$. This is only marginally higher than the contribution to the luminosity, reflecting that the contribution to H I mass density is basically flat and so only slightly affects the shape of the density distribution when the two are added together. LSB galaxies do have more of their baryons in the form of gas, as shown in the relationship between $M_{\rm H\,I}/L$ and surface brightness, but this is outweighed by their much lower luminosities.

If, in the usual way, we estimate the dynamical masses of HIDEEP galaxies using

$$M_{\rm dyn} = \frac{R_{\rm H\,I}(\Delta V_0)^2}{G}, \qquad (2)$$

where we follow Paper 1 in assuming $r_{\rm H\,I} \simeq 5\, r_{\rm e}$ and ΔV_0 is the inclination-corrected velocity width ($\Delta V_0 = \Delta V / \sin i$), then we arrive at the relative contribution of galaxies of various surface brightnesses shown in Fig. 13. For this calculation, only those galaxies with reliable inclinations in the range $45^\circ < i < 80^\circ$ were used. This leaves 57 galaxies in the HIMF-weighted sample and 38 in the $1/V_{\rm max}$-weighted sample. The share due to LSB galaxies is, although uncertain, relatively high at 22 ± 10 per cent for HIMF weighting or 21 ± 12 per cent for $1/V_{\rm max}$ weighting. This is in keeping with other studies that have shown that LSB galaxies contain proportionally more dark matter than normal galaxies.

Since the cross-sections of large, luminous galaxies can by no means explain the prevalence of quasar absorption-line systems (QSOALS), it has been suggested that LSB galaxies might be responsible (e.g. Phillipps, Disney & Davies 1993; Linder 1998, 2000), though this has proved controversial (e.g. Chen et al. 1998). If we assume that the absorption cross-sections of our galaxies are proportional to their effective areas (e.g. the area enclosed by the effective radius), then we can make an estimate of the contribution of LSB galaxies to this cross-section. Fig. 14 shows the cross-sectional area distribution of our galaxies with surface brightness (corrected to an inclination of 60°), formed in the same way as the above plots. This gives the contribution of LSB galaxies to the cross-section to be 39 ± 15 per cent using the HIMF weighting and 42 ± 22 per cent using $1/V_{\rm max}$ weighting.

Their high cross-section suggests that LSB galaxies are likely to form a significant fraction of the absorbers where galaxies themselves are responsible for QSOALS, as they might be in the case of damped Lyman α systems. This is borne out by recent observations where LSB galaxies, rather than HSB galaxies with immense haloes, appear to be the more likely absorbers (Turnshek et al. 2001; Bowen, Tripp & Jenkins 2001).

Table 4 summarizes the findings of this section. It can be seen that LSB galaxies make up over half of all gas-rich galaxies, yet have less than 10 per cent of the luminosity density. The relationship between dynamical M/L and surface brightness means that luminosity is a biased indicator of the cosmological significance of LSB galaxies. Similarly, the higher H I mass-to-light ratios of LSB galaxies mean that they have more gas than would be indicated by their light on a straight extrapolation of $M_{\rm H\,I}/L$ from Freeman-law galaxies. The relatively larger sizes of LSB galaxies means that their contribution to cross-sectional area, around 40 per cent, is much higher than would be expected from their luminosity or even from their H I mass.

The totals given here are only for galaxies with $M_{\rm H\,I} > 10^8\,{\rm M}_\odot$. These are almost entirely spiral galaxies. Dwarf galaxies, even gas-rich ones, tend to have lower gas masses than this, while elliptical galaxies are too gas-poor to be detected. Most dwarf galaxies have low surface brightnesses; therefore, if these were included, it is likely that the total contributions from LSB galaxies would rise. These numbers should therefore be seen as lower estimates for the total contribution of LSB galaxies.

Table 4. Summary of the measured contribution of HSB and LSB galaxies to the density of various quantities in gas-rich galaxies. These are the actual measured densities in the HIDEEP survey, for the SBDs constructed using weighting by the HIMF of Zwaan et al. (2003) and using $1/V_{\rm max}$ weighting. Possibly systematic errors due to the selection of the HIMF, calculated by comparing the results of the Zwaan et al. (2003) HIMF with other published HIMFs as described earlier, are given as a second error to the percentage LSB contribution.

Quantity	Weighting	$N_{\rm gal}$	HSB contribution	LSB contribution	Percentage LSB contribution
Number density	HIMF	101	1.8 ± 0.7	3.0 ± 1.5	$62 \pm 37^{+5}_{-3}$
(10^{-2} galaxies Mpc^{-3})	$1/V_{\rm max}$	62	2.9 ± 1.1	3.0 ± 0.9	51 ± 20
Neutral hydrogen density	HIMF	101	3.7 ± 0.7	1.8 ± 0.5	$32 \pm 11^{+10}_{-3}$
(10^7 M$_\odot$ Mpc^{-3})	$1/V_{\rm max}$	62	5.7 ± 1.2	2.1 ± 0.5	27 ± 7
Luminosity density	HIMF	101	45 ± 13	3.2 ± 1.0	$7 \pm 3^{+1}_{-1}$
(10^7 L$_\odot$ Mpc^{-3})	$1/V_{\rm max}$	62	57 ± 13	3.9 ± 1.2	7 ± 2
Baryon density	HIMF	101	68 ± 17	6.9 ± 2.1	$9 \pm 4^{+2}_{-1}$
(10^7 M$_\odot$ Mpc^{-3})	$1/V_{\rm max}$	62	88 ± 20	8 ± 2	9 ± 3
Mass density	HIMF	57	280 ± 80	77 ± 31	$22 \pm 10^{+4}_{-2}$
(10^7 M$_\odot$ Mpc^{-3})	$1/V_{\rm max}$	38	570 ± 170	150 ± 78	21 ± 12
Area density	HIMF	101	5.4 ± 1.2	3.4 ± 1.2	$39 \pm 15^{+8}_{-3}$
(10^{-1} kpc^2 Mpc^{-3})	$1/V_{\rm max}$	62	7.4 ± 1.7	5.4 ± 2.5	42 ± 22

5 CONCLUSIONS

This survey does not find any LSB 'crouching giant' galaxies, such as Malin 1. From this, we can rule out LSB galaxies making up more that 6 per cent of the population of luminous ($L_R > 10^{10}$ L$_\odot$) galaxies. Indeed, there does seem to be a minimum surface brightness at every magnitude level given approximately by $\mu_{\rm e,min} = 45 + M_R$ (Fig. 7). To higher surface brightnesses, galaxies seem to populate fairly evenly a band approximately four magnitudes wide in luminosity and two in surface brightness. Beyond this, high surface brightness, low-luminosity galaxies also appear to be rare in the gas-rich population. The populated band broadens slightly towards lower luminosities, giving it an approximate slope of $\Sigma \propto L^{0.7}$ (where Σ is surface brightness in luminosity per unit area and L is the total luminosity). From this, it can be calculated that the radius, R, is related to the surface brightness as $R \propto \Sigma^{0.2}$, i.e. the radius only changes very slightly with surface brightness.

Once volumetric corrections are made, the number of galaxies per unit volume is flat as we go to lower surface brightnesses. Even within the surface brightness limit reached by this survey, LSB galaxies contribute over half of the number density of galaxies. Furthermore, we find that LSB galaxies contribute approximately 30 per cent of the neutral hydrogen density, twice the lower limit set by Zwaan et al. (2003). LSB galaxies may also contribute around 20 per cent of the total mass density (again with large errors), but only 7 per cent of the luminosity density.

Overall, H I-rich LSB galaxies do not appear to contribute much to the Universe. However, the cross-section to QSOALS made by LSB galaxies, which is around 40 per cent of the total cross-section, is disproportionate to their luminosity or baryonic content. This implies that LSB galaxies could contribute substantially to those QSOALS where galaxies are the absorbers.

Future work in progress will see an order-of-magnitude larger sample assembled from the overlap between HIPASS and the SDSS. This will give not only an increase in the significance of the results, but also five-colour optical data, thus greatly extending our knowledge of H I-selected galaxies. A larger sample of H I-selected samples from the SDSS may be assembled in the medium term by the proposed ALFALFA drift-scan survey with the Arecibo *L*-band Feed Array or in the longer term by surveys carried out with the Square Kilometre Array. However, as neither HIPASS nor ALFALFA reach column density levels as low as HIDEEP, it is unlikely that they will turn up any significant population of extremely LSB galaxies that we have missed.

This is not to say that extremely LSB galaxies do not exist, just that, if they do make up a significant population, then the amount of H I they contain must be small. In order to search for these galaxies, techniques other than H I surveys will be necessary. The optical channel available to us on the ground is fundamentally unsuited to looking for LSB galaxies, but a quite modest switch in wavelengths to either side of the solar peak, which is possible from space, could yield dramatic results. O'Connell (1987) has discussed the idea of using ultraviolet wavelengths, while in the *H* band at 1.6 μm the contrast between the Sun's scattered zodiacal spectrum and the light from red stars in LSB galaxies could be two orders of magnitude higher than the contrast from the ground. Wide-field near-infrared cameras, such as the WFC-3 instrument currently awaiting shipment to the *HST*, will be needed to exploit this window, which is, in principle, capable of revealing galaxies 7 mag lower in surface brightness than we can detect from the ground.

ACKNOWLEDGMENTS

The authors would like to thank Lister Staveley-Smith, Tony Fairall, David Barnes, Jon Davies and Suzanne Linder for useful discussions. RFM, WJGdeB and PJB acknowledge the support of PPARC. BKG acknowledges the support of the Australian Research Council. The authors would also like to thank the staff of the CSIRO Parkes and Narrabri Observatories, of the NRAO Array Operations Center and of the ANU Siding Spring Observatory for their help with observations. We acknowledge PPARC grant GR/K/28237 to MJD towards the construction of the multibeam system and PPARC grants PPA/G/S/1998/00543, PPA/G/S/1998/00620, PPA/G/S/2002/00053 and PPA/G/S/2003/00085 to MJD towards its operation. We would particularly like to thank the anonymous referee for an extremely helpful report.

This research has made use of the NASA/IPAC Extragalactic Database (NED), which is operated by the Jet Propulsion

Laboratory, Caltech, under agreement with the National Aeronautics and Space Administration. This research has also made use of the Digitised Sky Survey, produced at the Space Telescope Science Institute under US Government Grant NAG W-2166 and of NASA's Astrophysics Data System Bibliographic Services.

REFERENCES

Barnes D. G. et al., 2001, MNRAS, 322, 486
Bertins E., Arnouts S., 1996, A&AS, 117, 393
Bland-Hawthorn J., Shopbell P. L., Malin D. F., 1993, AJ, 106, 2154
Blanton M. R. et al., 2001, AJ, 121, 2358
Bowen D. V., Tripp T. M., Jenkins E. B., 2001, AJ, 121, 1456
Boyce P. J., Phillipps S., 1995, A&A, 296, 26
Briggs F. H., Rao S., 1993, ApJ, 417, 494
Chen H.-W., Lanzetta K. M., Webb J. K., Barcons X., 1998, ApJ, 498, 77
Churchill C. W., Le Brun V., 1998, ApJ, 499, 677
Davies J. I., 1990, MNRAS, 244, 8
de Blok W. J. G., McGaugh S. S., van der Hulst J. M., 1996, MNRAS, 283, 18
de Jong R. S., 1996a, A&A, 313, 45
de Jong R. S., 1996b, A&A, 313, 377
Disney M. J., 1976, Nat, 263, 573
Disney M. J., 1999, in Davies J. I., Impey C., Phillipps S., eds, ASP Conf. Ser. Vol. 170, The Low Surface Brightness Universe. Astron. Soc. Pac., San Francisco, p. 9
Disney M. J., Phillipps S., 1983, MNRAS, 205, 1253
Driver S. P., 1999, ApJ, 576, L69
Freeman K. C., 1970, AJ, 160, 811
Fukugita M., Hogan C. J., Peebles P. J. E., 1998, ApJ, 503, 518
Graham A. W., de Blok W. J. G., 2001, ApJ, 556, 177
Hambly N. C. et al., 2001, MNRAS, 326, 1279
Henning P. A. et al., 2000, AJ, 119, 2686
Impey C. D., Bothun G. D., 1997, ARA&A, 35, 367
Kilborn V. A., 2001, PhD thesis, Univ. Melbourne
Koribalski B. S. et al., 2004, AJ, 128, 16
Kron R. G., 1980, ApJS, 43, 305
Lauberts A., Valentijn E. A., 1989, The Surface Photometry Catalogue of the ESO-Uppsala Galaxies. ESO, Garching
Linder S. M., 1998, ApJ, 495, 637
Linder S. M., 2000, ApJ, 529, 644
McGaugh S. S., 1996, MNRAS, 280, 337
McGaugh S. S., Schombert J. M., Bothun G. D., de Blok W. J. G., 2000, ApJ, 533, 99
Maddox S. J., Efstathiou G., Sutherland W. J., 1990, MNRAS, 246, 433
Masters K. L., Haynes M. P., Giovanelli R., 2004, ApJ, 607, L115
Minchin R. F., 1999, PASA, 16, 12
Minchin R. F. et al., 2003, MNRAS, 346, 787 (Paper 1)
O'Connell R., 1987, AJ, 94, 867
Parker Q. A., Malin D. F., 1999, PASA, 16, 288
Phillipps S., Disney M. J., Davies J. I., 1993, MNRAS, 260, 453
Rosenberg J. L., Schneider S. E., 2002, ApJ, 567, 247
Ryan-Weber E. et al., 2002, AJ, 124, 1954
Schlegel D. J., Finkbeiner D. P., Davis M., 1998, ApJ, 500, 525
Schneider S. E., Spitzak J. G., Rosenberg J. L., 1998, ApJ, 507, 9
Thim F., Tammann G. A., Saha A., Dolphin A., Sandage A., Tolstoy E., Labhardt L., 2003, ApJ, 590, 256
Turnshek D. A., Rao S., Nestor D., Lane W., Monier E., Bergeron J., Smette A., 2001, ApJ, 553, 288
Zwaan M. A., van der Hulst J. M., de Blok W. J. G., McGaugh S. S., 1995, MNRAS, 273, L35
Zwaan M. A., Briggs F. H., Sprayberry D., Sorar E., 1997, ApJ, 490, 173
Zwaan M. A. et al., 2003, AJ, 125, 2842

This paper has been typeset from a TEX/LATEX file prepared by the author.